applied sciences

MDPI

Communication

Optimization Tools for the Design of Meta-Covers for Linear Antenna with Beam- and Null-Steering Capabilities

Michela Longhi [1,*], Stefano Vellucci [1], Mirko Barbuto [2], Alessio Monti [2], Filiberto Bilotti [2] and Alessandro Toscano [2]

[1] Department of Engineering, Niccolò Cusano University, Via Don Carlo Gnocchi, 3, 00166 Rome, Italy
[2] Department of Industrial, Electronic and Mechanical Engineering, Roma Tre University, Via Vito Volterra, 62, 00146 Rome, Italy
* Correspondence: michela.longhi@unicusano.it

Abstract: This paper investigates the optimization of cylindrical metasurface meta-covers designed to enable beamforming capabilities in single linear antennas. This study focuses on the development and application of advanced optimization tools to tailor the electromagnetic response of these metasurfaces, enabling precise control over the radiation patterns of the antenna. In particular, we develop a genetic algorithm-based optimization tool, which achieves precise manipulation of the main beam direction and null placement in the radiation pattern. The results further expand the applications of metasurface-based meta-covers in enhancing the functionality of dipole antennas in various communication and sensing systems.

Keywords: metasurface; beamforming; null-steering; genetic algorithm

check for updates

Academic Editor: John Xiupu Zhang

Received: 31 October 2024
Revised: 12 December 2024
Accepted: 7 January 2025
Published: 8 January 2025

Citation: Longhi, M.; Vellucci, S.; Barbuto, M.; Monti, A.; Bilotti, F.; Toscano, A. Optimization Tools for the Design of Meta-Covers for Linear Antenna with Beam- and Null-Steering Capabilities. *Appl. Sci.* **2025**, *15*, 553. https://doi.org/10.3390/app15020553

Copyright: © 2025 by the authors. Licensee MDPI, Basel, Switzerland. This article is an open access article distributed under the terms and conditions of the Creative Commons Attribution (CC BY) license (https://creativecommons.org/licenses/by/4.0/).

1. Introduction

Pattern reconfigurable antennas are essential for mitigating noise and interference, overcoming jamming signals, and enhancing system gain. By directing signals exclusively toward desired directions, these antennas also conserve energy and increase user capacity [1,2]. They are crucial for the next generations of mobile communication, including 5G, beyond 5G, and future 6G networks, supporting location-based services for the mobile Internet [3,4].

To effectively address complex environments and increasingly sophisticated demands, reconfigurable antennas must not only be versatile but also highly precise in their operation. This precision is essential for adapting to the dynamic conditions of modern communication systems. Beam-steering antenna systems, in particular, have garnered significant interest due to their ability to provide interference-free, power-efficient, and highly secure end-to-end communication [5–8]. Moreover, by incorporating null-steering capabilities, a beam-steering reconfigurable antenna can also generate one or more nulls in specific directions [9]. This feature is especially valuable as it allows the antenna to direct nulls toward interfering or jamming signals, thereby enhancing the signal-to-noise ratio and improving connection stability and reliability [10].

Although several designs achieving effective null-steering have been developed in the literature, challenges such as limited bandwidth, high computational complexity, and reliance on large arrays still persist [11,12]. Significant advancements have been made in null-steering antenna technologies for precise null-steering applications [13], including metasurface-based antennas that enable beamforming and steering with high efficiency [14,15]. Additionally, the integration of metasurface structures into computational

imaging systems for enhanced control of electromagnetic wave manipulation has been achieved [16]. Despite these contributions, challenges remain, including the reliance on complex configurations, limitations in achieving precise null placement across varying operational scenarios, and scalability issues. Our work addresses these gaps by introducing cylindrical metasurface meta-covers optimized through a genetic algorithm. This approach offers precise control over both beam direction and null placement while maintaining a compact and efficient design. Our results demonstrate enhanced radiation pattern manipulation, enabling broader applications in communication and sensing systems.

The most common implementation for null-steering antennas is using arrays of N elements fed by a beamforming network (BFN) to generate $N - 1$ scannable nulls [17]. While these techniques offer high performance, they are often hindered by the need for extensive arrays, multiple sensors or channels, intensive computation, and costly hardware [18–20].

In this context, metasurfaces that cover antennas have emerged as a transformative technology, enabling advanced functionalities in communication systems [21]. These ultra-thin, planar structures can manipulate electromagnetic waves in ways that were previously unattainable with conventional materials. Metasurfaces are engineered structures composed of subwavelength elements that can locally control the amplitude, phase, and polarization of electromagnetic waves with a precision that is not achievable with conventional bulk materials. This capability arises from their ability to impose abrupt, spatially varying boundary conditions on the propagating wavefront, enabling functionalities such as beam steering, polarization conversion, and wavefront shaping. Unlike conventional materials, whose electromagnetic properties are governed by constitutive parameters, i.e., permittivity and permeability, metasurfaces rely on the geometric design and arrangement of their constituent elements, offering unparalleled flexibility in wave manipulation. Regarding the manipulation of the radiation patterns, recent research based on magnetic meta-atoms has realized the nonreciprocal unidirectional scattering [22] and the nonreciprocal Kerker effect [23]. When applied to antennas, metasurfaces can enhance performance, for instance, by providing dynamic control over the radiation patterns, allowing for precise beam-steering. However, conventional approaches often require redesigning individual radiating elements within the antenna array, which can limit their flexibility and adaptability. To address these limitations, reconfigurable intelligent metasurfaces are employed, offering a solution that allows for dynamic beam manipulation without the need for extensive modifications to existing antenna structures [24]. This beam-steering approach offers a more pragmatic and cost-effective solution than conventional antennas. Indeed, antennas enhanced by metasurfaces feature simple design elements, and passive beam scanning capabilities eliminate the need for power-hungry and complex active RF components [25,26]. As a result, research on these antenna systems is advancing rapidly to meet the growing mass-market demand for low-cost, low-profile beam-steering front-end devices. While this approach has demonstrated its effectiveness, current studies have yet to fully explore the wide range of degrees of freedom offered by metasurfaces. So far, most studies have focused on controlling only a few radiation pattern characteristics, such as the main beam direction [27–29]. Indeed, in our previous works, we demonstrated that metasurface coatings on linear dipole antennas can shape the antenna's radiation pattern by controlling the position of the main lobes [30]. More recently, we have shown that metasurface synthesis could be efficiently performed by leveraging a circular array model [25]. However, a key aspect that remains underexplored in these early works involving metasurfaces is their ability to enable effective sidelobe control and suppression of unwanted signals. While null-steering has been extensively studied in traditional antenna arrays, our work aims to address this gap by harnessing the potential of metasurfaces to

optimize both the main beam and null positioning in the radiation pattern, employing an evolutionary algorithm as a novel approach for these configurations.

Building on these advancements, this paper introduces a novel design of a cylindrical Huygens metasurface (HMS) surrounding a dipole antenna optimized through a Genetic Algorithm (GA) to improve the metasurface parameters for beamforming and null-steering applications. The GA-driven optimization is a key innovation that allows for the precise tuning of metasurface parameters. Unlike prior works, which primarily focus on beam direction, our approach introduces the control to place nulls in the radiation pattern at exact and predefined positions. This unprecedented level of precision marks a significant advancement in this field.

The adaptation of methods traditionally used for rectangular antenna arrays to cylindrical geometries requires significant modifications due to the inherent differences in boundary conditions and geometry. In this work, we have extended the concept of array synthesis by carefully modifying the analysis to account for the geometry of cylindrical arrays. This study of cylindrical antenna arrays is well-established, as seen in numerous publications that have analyzed their radiation characteristics and synthesis techniques [31,32]. For example, some studies have explored the opportunities associated with cylindrical geometry, such as its impact on mutual coupling and array factor computations [33]. However, this work aims to integrate cylindrical metasurfaces with optimization algorithms to enable precise control of beamforming and null-steering. By leveraging metasurface technologies, which are less explored in the context of cylindrical geometries, this work contributes to bridging the gap between conventional array analysis and modern metasurface-based antenna designs.

Finally, the scalability of the GA-based optimization method can be constructed to address its applicability to higher frequencies and varying operating conditions. Specifically, the flexibility of the GA allows for seamless adaptation to different frequency bands, including those relevant to emerging technologies such as 5G and 6G. This is achieved by tuning the design constraints to account for higher operating frequencies and optimizing the metasurface parameters to support broader bandwidths and enhanced performance metrics. Furthermore, the inherent adaptability of the GA enables it to address varying operational scenarios, such as changes in beamforming requirements or environmental conditions, without significant modifications to the optimization framework. These features make the proposed method suitable for dynamic and scalable antenna system designs, ensuring its utility for future wireless communication systems.

The structure of this paper is as follows: Section 2 provides a detailed explanation of the HMS design process, focusing on the use of GA optimization. Specifically, it examines the mechanism behind beam- and null-steering and utilizes the developed model to optimize cylindrical HMSs for wire antenna coatings. Section 3 showcases various configurations designed and modeled using the proposed approach, with the corresponding results compared against those obtained through full-wave numerical simulations. Finally, the conclusions summarize the main findings and outline potential future research directions.

2. Circular Array Synthesis Approach

Steering a transmitted beam in a desired direction is a critical function in telecommunication systems, enabling targeted coverage of specific areas within the surrounding environment. Traditionally, phased antenna arrays have been used to achieve this [34]. However, these systems depend on complex phase-shifting networks, which are often energy-intensive and can lead to signal losses [35–37].

A novel approach to overcoming these limitations involves the use of metamaterial covers and coatings, which offer an alternative design strategy by introducing abrupt phase

variations in the transmitted wave [30]. In particular, we focus on the specific class of HMS, a type of engineered surface that uses arrays of subwavelength elements to achieve precise control of electromagnetic waves, including manipulation of phase, amplitude, and polarization, based on Huygens' principle of wavefront shaping. HMSs are composed of unit cells that ensure full transmission and allow for precise control over the phase of the transmitted field by aligning electric and magnetic dipole moments [38–40]. The flexibility provided by the Huygens cells makes it possible to fine-tune the antenna's performance in dynamic environments, enhancing its effectiveness in targeted communication and noise reduction. A straightforward way to synthesize the HMS cells relies on the use of stacked impedance sheets separated by dielectric layers, characterized by a surface impedance value $Z_{s,ni}$, where $i = 1, 2, 3\ldots$ represents the number of stacked layers [19]. This configuration ensures high transmission values and phase coverage that strongly depends on the thickness of the dielectric layer [41]. In our specific case, we have chosen three metasurface layers and two thin dielectric substrates. The substrate has a thickness $t = \lambda_0/60$ and a relative permittivity $\varepsilon_r = 10$, while $Z_{s,ni}$ is assumed to be purely reactive (i.e., $Z_{s,ni} = jX_{s,ni}$ with j being the imaginary unit) in the range $[-990, +100]\ \Omega/\text{sq}$.

In this work, the HMS coating structure is designed in Figure 1a.

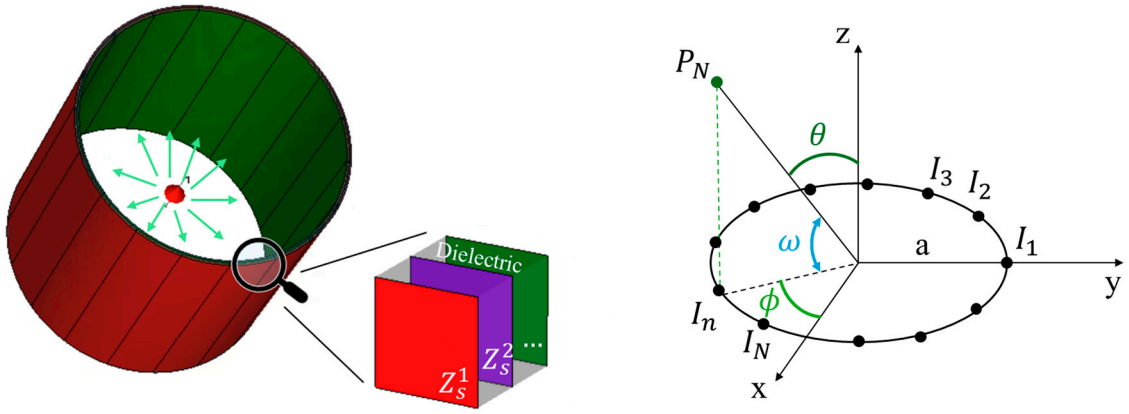

(**a**) (**b**)

Figure 1. (**a**) Design of the HMS coating of the omnidirectional antenna. In the inset are the details of the unit cell implementing the HMS, which consists of stacked impedance sheets separated by dielectric layers. (**b**) Equivalent circular array model used for the metasurface synthesis procedure.

In [25], we have shown that for the synthesis of the metasurface, the cylindrical HMS can be segmented into N cells, with each cell functioning as an individual antenna element in an equivalent circular array, as depicted in Figure 1b. We propose to design the cylindrical metasurfaces by leveraging the synthesis techniques of circular antenna arrays. Specifically, the cylindrical metasurface is treated as operating in the H-plane, making its behavior analogous to that of a circular array. This methodology allows for the simplification of the metasurface synthesis process while enabling precise control over the radiation characteristics. In this way, the HMS can be described through the synthesis of a circular array consisting of N elements with a radius a on the xy-plane. This correspondence allows for the effective representation and manipulation of the HMS's electromagnetic behavior by treating it as an array, facilitating precise control over its phase and amplitude characteristics. In this modeling scenario, the total electric field expression of the circular array is defined as the field of a single radiating element multiplied by the array factor AF that reads as (Equation (1)):

$$AF(\theta,\phi) = \sum_{n=1}^{N} I_n e^{j[ka\ sin\theta cos(\phi-\phi_n)+\alpha_n]}, \quad (1)$$

In particular, I_n represents the excitations amplitude, while α_n describes the excitation phases of the array elements, and it is expressed as $\alpha_n = -ka\ sin\theta_0\ cos(\phi_0 - \phi_n)$ when the array points toward (θ_0, ϕ_0) direction. For the evaluation of the total radiated field distribution, one must also consider the element factor of the cell, where the single Huygens cell exhibits a directive radiation pattern, as given by the following Equation (2) [26]:

$$g_n(\theta,\varphi) = \begin{cases} \cos(\phi-\phi_n) & -90^\circ < \phi < 90^\circ \\ 0 & otherwise \end{cases}. \quad (2)$$

In Equation (2), ϕ denotes the azimuth angle measured from the positive x-axis, while ϕ_n specifies the angular position of the n-th element within the xy-plane. The elevation angle θ is defined with respect to the positive z-axis, as illustrated schematically in Figure 1b.

This directive behavior affects the overall radiation characteristics of the metasurface, and accounting for it is essential to accurately model the performance of the entire structure. By integrating the element pattern into the synthesis, we ensure that the individual contributions of each Huygens cell are properly accounted for, leading to a more precise and effective beamforming design. After deriving the expressions for the cell element pattern and the array factor, the complete array pattern is given by

$$AP(\theta,\varphi) = AF(\theta,\varphi)\ g_n(\theta,\varphi). \quad (3)$$

Although the beamforming capabilities and the underlying physical principles of this design approach were demonstrated in our previous works, not all the design possibilities offered have been investigated. To further enhance the capabilities of the overall system, in this paper, we employ an evolutionary optimization method of the metasurface parameters, specifically a GA. This approach allows for improved control over the radiation pattern, addressing the requirements of both the main beam and radiation null directions.

3. Genetic Algorithm Optimization

With the HMS synthesis method presented in the previous section, it is possible to fix the position of one or more main lobes. However, to achieve more precise control over both the intensity of these lobes and the position of the nulls, optimization techniques are implemented. These techniques allow for fine-tuning of the radiation pattern, ensuring that both the desired beam directions and null locations are accurately achieved, improving the overall performance of the antenna. The objective of this optimization is to configure the radiation pattern as closely as possible to the desired outcome. To achieve an optimal configuration, nulls are imposed at specific angles in the radiation pattern while keeping the main beam position fixed. Constraints are applied to maintain the desired directivity in both the null and main beam directions. The key advantage of using a GA lies in its ability to efficiently search for integer solutions, which narrows the configuration space and accelerates convergence. Once the GA determines the required phase shifts for each metasurface element to achieve the desired radiation pattern, the corresponding surface reactances are calculated to match these phase values. This ensures that the metasurface is precisely designed to deliver the desired radiation characteristics.

The workflow presented in the diagram of Figure 2 outlines the optimization process for synthesizing a circular HMS structure. It begins with the modeling of a circular antenna array in MATLAB (version R2024b), where the radiating elements are designed to emulate the behavior of a HMS with zero phase shift and a unitary transmission coefficient. The

initial step involves the synthesis of the circular array exploiting Equation (1), which provides directivity values for the main lobe. These preliminary directivity values are then enhanced through the implementation of GA optimization. Specifically, it is necessary to define input data, including the initial HMS structure derived from a circular array synthesis and the desired main beam direction and null positions. The GA optimization is employed to iteratively adjust the directivity and null values, targeting convergence based on predefined criteria such as tolerance thresholds and maximum iterations. The switching criterion ensures that the optimization loop continues until these conditions are satisfied, i.e., the optimization targets a +20 dB directivity for the main lobe and a −20 dB for the nulls at the specified angle. Once convergence is achieved, the output consists of the calculated reactance values for each HMS cell, which are then used to finalize the metasurface design. This workflow provides a systematic approach to achieving precise null-steering and optimal radiation characteristics using metasurface technology.

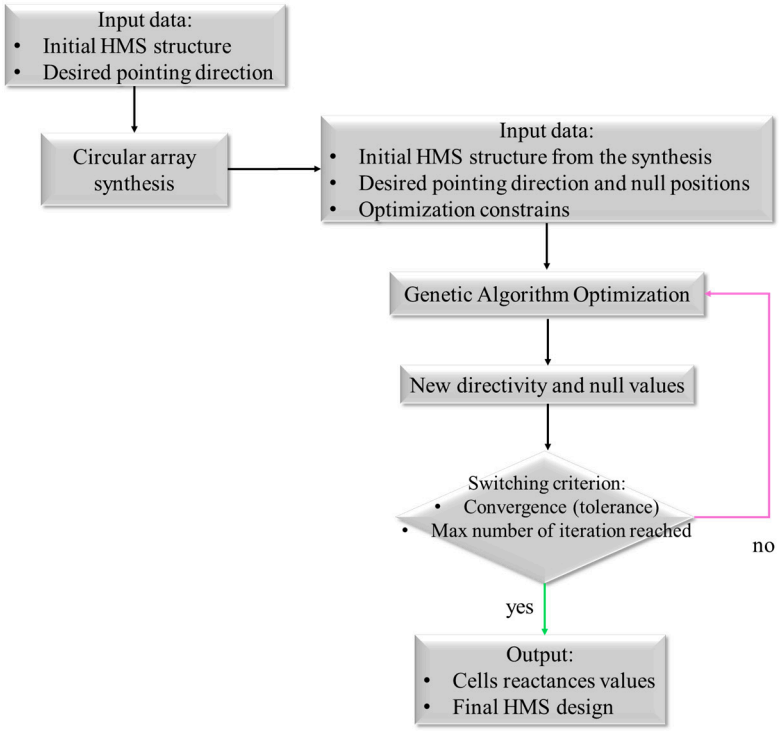

Figure 2. Flowchart of the GA optimization for metasurface design.

4. Discussion and Results

To improve the performance of the array synthesis approach, multiple optimization runs utilizing genetic algorithm strategies were implemented. These runs facilitate the search for the optimal solution across the entire configuration space. In this case, the optimal solution is defined by a set of N = 18 phase shifts, each assigned to an individual cell element, in order to generate the desired radiation pattern. Based on the results obtained, the MATLAB code calculates the correct values required for each metasurface cell, as shown in Figure 1a, ensuring accurate implementation in a full-wave simulation.

To evaluate the effectiveness of the proposed design approach, we analyzed the performance of the GA-optimized configuration. Figure 3a shows the 2D far-field plot of the normalized directivity on the H-plane of the antenna, comparing the results obtained through the approach based on the simple circular array synthesis (blue line) [26] with the enhanced approach based on the Genetic Algorithm optimization. The main lobe directions are set at 30°, 45°, and 60°, with nulls imposed at corresponding angles to avoid high-side lobes. The corresponding values of the maximum main lobe and null positions for each

configuration are presented in Table 1, further validating the effectiveness of the proposed optimization method across various configurations.

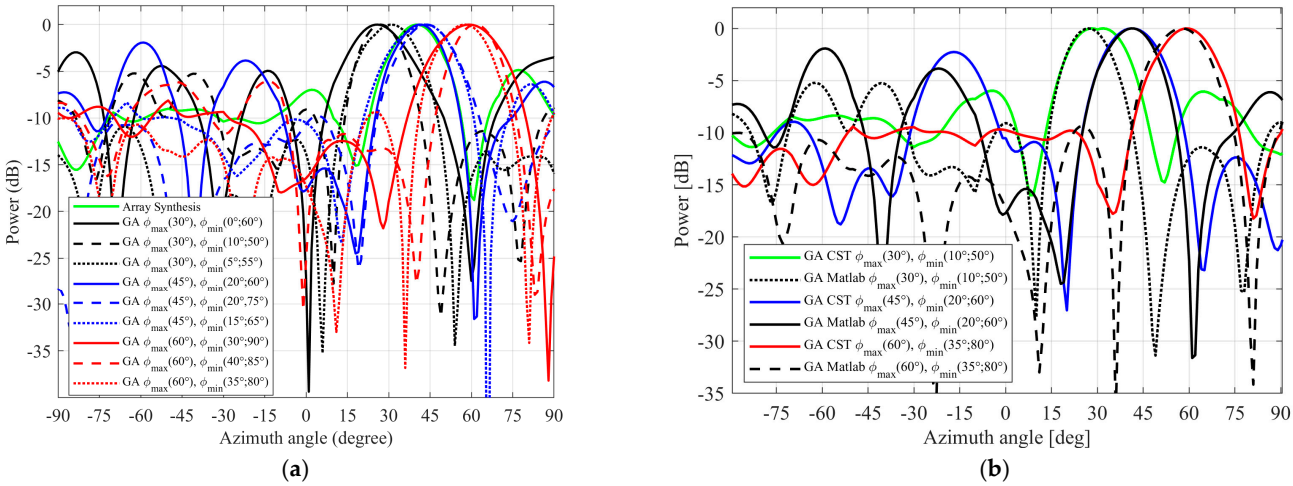

Figure 3. (**a**) Normalized far-field directivity results of the HMS pattern by circular array synthesis code (green line) for main lobe at 45° and nulls at 20° and 60°, and GA code (other lines), evaluated at 0° of elevation angle. (**b**) Comparison between CST electromagnetic simulation and MATLAB estimation illustrating the results for multiple main lobe directions and null directions.

Table 1. Corresponding values of the maximum main lobe and null positions for each configuration of Figure 3a.

Max Main Lobe	First Null	Second Null
30°	0°	60°
	5°	55°
	10°	50°
45°	15°	65°
	20°	60°
	20°	75°
60°	30°	90°
	35°	80°
	40°	85°

Additionally, to assess the feasibility of adopting the proposed GA algorithm for dynamically adjusting the behavior of the HMS. The GA was chosen for its flexibility and adaptability in handling the specific constraints of our metasurface design. The optimization process is applied to a structure that has already been initialized with a synthesis performed using the circular array model. This initial step significantly reduces the computational complexity, allowing the algorithm to focus on fine-tuning the structure for the desired radiation properties. This result highlights the potential for real-time adaptation, although future improvements could focus on reducing this computation time to enhance the system's dynamic responsiveness in practical applications. The computational time is a significant improvement compared to traditional gradient-based methods [22], which often require multiple iterations over complex cost functions, leading to longer runtimes. However, real-time applications demand further reduction in computational complexity. Future optimizations could explore parallelization techniques or hybrid algorithms to enhance performance while maintaining accuracy.

We finally compare the semi-analytically derived results with a full-wave EM simulation tool. Hereinafter, without losing generality, the case of a coating metasurface

characterized by a radius $a = \lambda_0/2$ and operating frequency $f_0 = 2.6$ GHz is considered. For clarity and readability, we present one representative case for each main lobe direction in Figure 3b. The directivity pattern of the GA manipulation is compared to the radiation pattern coming from the design of an HMS structure obtained with the full-wave simulations. A very good matching between the two curves can be observed, particularly regarding the maximum and minimum positions. The GA model accurately predicts the shape of the radiation pattern, the beamwidth, and the sidelobe levels. Thanks to this approach, it is possible to calculate the maximum directivity value (i.e., the ratio of the maximum radiation intensity in a given direction to the average radiation intensity over all directions), which is 8.19 dB, in a very fast and easy way. The value of 8.19 dB was obtained from the optimized radiation pattern computed through the genetic algorithm. This process involved maximizing the radiation intensity in the desired direction based on the excitation phases and amplitudes of the array.

The results obtained by implementing the GA demonstrated significantly greater precision in controlling the position of the main beam and nulls compared to conventional methods. To further corroborate the results, in Figure 4, we report the 3D radiation pattern of the antenna coated by the HMS designed through the circular array approach (Figure 4a) and after the GA optimization (Figure 4b). By effectively utilizing GA optimization, improvements in both beam-steering and null-steering can be observed in the final radiation pattern of the structure.

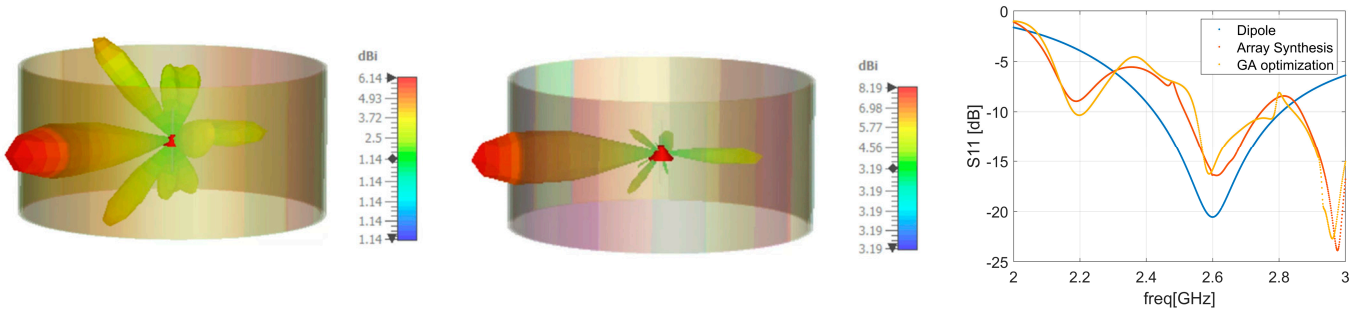

(**a**) (**b**) (**c**)

Figure 4. A 3D directivity radiation pattern of the HMS structure (**a**) before and (**b**) after the GA optimization. (**c**) Magnitude of the reflection coefficient at the antenna input port for the scenarios w/o (blue line) and w/(red and yellow lines) the optimization for the HMS coating.

Finally, it is worth noting that despite the introduction of the HMS coating, the matching performance of the dipole antenna remains quite good, as demonstrated in Figure 4c. The figure compares the reflection coefficient magnitude at the antenna input port with that of the same structure but different values of HMS cell's reactances corresponding to the cases of the circular synthesis approach and with the GA optimization procedure.

While the proposed metasurface design demonstrates promising simulation results, practical implementation involves several challenges that must be addressed. First, the selection of suitable materials with precise electromagnetic properties is critical to achieving the desired performance. Second, manufacturing tolerances, particularly for subwavelength-scale features of the metasurface, can introduce deviations from the ideal design. Third, integration of the metasurface with existing antenna systems requires careful mechanical and electrical considerations. Future work will explore these aspects to ensure the feasibility of the proposed design in real-world applications.

5. Conclusions

In this work, we presented an optimized cylindrical metasurface design enabling precise beamforming and null-steering through a genetic algorithm-based approach. The proposed method provides a flexible and computationally efficient solution for tailoring radiation patterns in cylindrical geometries. Future research will focus on extending the design for higher-frequency bands, including 5G and 6G, as well as addressing fabrication challenges to facilitate experimental validation. A key contribution of this work is the use of a GA optimization tool combined with a rigorous model of individual HMS unit cells acting as radiating elements in an equivalent circular array. This approach allows for the precise analytical derivation of the phase-insertion values of the HMS cells, enabling accurate steering of both the main beam and nulls to the desired directions.

The proposed model significantly enhances the potential applications of HMS coatings in controlling the radiation characteristics of wire antennas. It enables a comprehensive synthesis of the radiation pattern, paving the way for advanced manipulation of antenna performance. Moreover, by integrating the GA-based approach, this method introduces a novel pathway for the design of reconfigurable antennas, particularly suited for next-generation communication systems where precise beam and null control is critical.

Author Contributions: Writing—original draft, M.L., S.V., M.B., A.M., F.B. and A.T. All authors have read and agreed to the published version of the manuscript.

Funding: This research has been developed in the frame of the activities of the research contract: "MEETAPP" PRIN 2022 project (protocol number 2022ZZ8APA), funded by the Italian Ministry of University and Research.

Institutional Review Board Statement: Not applicable.

Informed Consent Statement: Not applicable.

Data Availability Statement: The original contributions presented in the study are included in the article, further inquiries can be directed to the corresponding author.

Conflicts of Interest: The authors declare no conflict of interest.

References

1. Ojefors, E.; Cheng, S.; From, K.; Skarin, I.; Hallbjorner, P.; Rydberg, A. Electrically-steerable single-layer microstrip traveling wave antenna with varactor diode based phase shifters. *IEEE Trans. Antennas Propag.* **2007**, *55*, 2451–2460. [CrossRef]
2. Topak, E.; Hasch, J.; Wagner, C.; Zwick, T. A novel millimeter-wave dual-fed phased array for beam steering. *IEEE Trans. Microw. Theory Tech.* **2013**, *61*, 3140–3147. [CrossRef]
3. Liao, B.; Chan, S.C. Direction finding with partly calibrated uniform linear arrays. *IEEE Trans. Antennas Propag.* **2012**, *60*, 922–929. [CrossRef]
4. Zhou, R.; Zhang, H.; Xin, H. Improved two-antenna direction finding inspired by human ears. *IEEE Trans. Antennas Propag.* **2011**, *59*, 2691–2697. [CrossRef]
5. Law, D.C.; McLaughlin, S.A.; Post, M.J.; Weber, B.L.; Welsh, D.C.; Wolfe, D.E.; Merritt, D.A. An electronically stabilized phased array system for shipborne atmospheric wind profiling. *J. Atmos. Ocean. Technol.* **2002**, *19*, 924–933. [CrossRef]
6. Jayakrishnan, V.M.; Vijayan, D.M. Performance analysis of smart antenna for marine communication. In Proceedings of the 2020 2nd International Conference on Innovative Mechanisms for Industry Applications (ICIMIA), Bangalore, India, 5–7 March 2020; pp. 88–91.
7. Flores-Vidal, X.; Flament, P.; Durazo, R.; Chavanne, C.; Gurgel, K.-W. High-frequency radars: Beamforming calibrations using ships as reflectors. *J. Atmos. Ocean. Technol.* **2013**, *30*, 638–648. [CrossRef]
8. Lockie, D.G.; Sereno, M.; Thomson, M. Spacecraft Antennas and Beam Steering Methods for Satellite Communication System. U.S. Patent 5 642 122, 24 June 1997.
9. Ross, G.; Schwartzman, L. Continuous beam steering and null tracking with a fixed multiple-beam antenna array system. *IEEE Trans. Antennas Propag.* **1964**, *12*, 541–551. [CrossRef]

10. Shmuel, O.; Cohen, A.; Gurewitz, O. Multi-Antenna Jamming in Covert Communication. *IEEE Trans. Commun.* **2021**, *69*, 4644–4658. [CrossRef]
11. Pal, A.; Mehta, A.; Skippins, A.; Spicer, P.; Mirshekar-Syahkal, D. Novel Interference Suppression Null Steering Antenna System for High Precision Positioning. *IEEE Access* **2020**, *8*, 77779–77787. [CrossRef]
12. Tamura, J.; Arai, H. Simple and Accurate Received Signal Strength-Based Localization Using Compact Null-Steering Antennas. *IEEE Antennas Wirel. Propag. Lett.* **2023**, *22*, 417–421. [CrossRef]
13. Tamura, J.; Arai, H.; Itoh, T. High-Impedance Surface-Based Null-Steering Antenna for Angle-of-Arrival Estimation. *IEEE Trans. Antennas Propag.* **2022**, *70*, 3269–3276. [CrossRef]
14. Ahmed, F.; Singh, K.; Esselle, K.P. State-of-the-Art Passive Beam-Steering Antenna Technologies: Challenges and Capabilities. *IEEE Access* **2023**, *11*, 69101–69116. [CrossRef]
15. Yang, W.; Li, J.; Chen, D.; Cao, Y.; Xue, Q.; Che, W. Advanced Metasurface-Based Antennas: A review. *IEEE Open J. Antennas Propag.* **2024**. [CrossRef]
16. Imani, M.F.; Gollub, J.N.; Yurduseven, N.; Diebold, A.V.; Boyarsky, M.; Fromenteze, T.; Pulido-Mancera, L.; Sleasman, T.; Smith, D.R. Review of Metasurface Antennas for Computational Microwave Imaging. *IEEE Trans. Antennas Propag.* **2020**, *68*, 1860–1875. [CrossRef]
17. Dicandia, F.A.; Genovesi, S.; Monorchio, A. Null-Steering Antenna Design Using Phase-Shifted Characteristic Modes. *IEEE Trans. Antennas Propag.* **2016**, *64*, 2698–2706. [CrossRef]
18. Van Veen, B.D.; Buckley, K.M. Beamforming: A versatile approach to spatial filtering. *IEEE ASSP Mag.* **1988**, *5*, 4–24. [CrossRef] [PubMed]
19. Yang, J.; Lu, J.; Liu, X.; Liao, G. Robust null broadening beamforming based on covariance matrix reconstruction via virtual interference sources. *Sensors* **2020**, *20*, 1865. [CrossRef]
20. Zhu, L.; Ma, W.; Zhang, R. Movable-Antenna Array Enhanced Beamforming: Achieving Full Array Gain with Null Steering. *IEEE Commun. Lett.* **2023**, *27*, 3340–3344. [CrossRef]
21. Bilotti, F.; Barbuto, M.; Hamzavi-Zarghani, Z.; Karamirad, M.; Longhi, M.; Monti, A.; Ramaccia, D.; Stefanini, L.; Toscano, A.; Vellucci, S. Reconfigurable intelligent surfaces as the key-enabling technology for smart electromagnetic environments. *Adv. Phys. X* **2024**, *9*, 2299543. [CrossRef]
22. Liu, M.Q.; Zhao, C.Y.; Wang, B.X. Active tuning of directional scattering by combining magneto-optical effects and multipolar interferences. *Nanoscale* **2018**, *10*, 18282–18290. [CrossRef]
23. Chen, Y.; Zhang, Y.; Ba, Q.; Zhao, L.; He, J.; Zhang, L.; Luo, Q.; Liu, S. ENZ medium triggered collapse of Fano resonances and emergence of generalized nonreciprocal Kerker effects by subwavelength hybrid meta-atoms. *Phys. Rev. B* **2023**, *108*, 235413. [CrossRef]
24. Vellucci, S.; Monti, A.; Barbuto, M.; Longhi, M.; Hamzavi-Zarghani, Z.; Ramaccia, D.; Stefanini, L.; Toscano, A.; Bilotti, F. Meta-Covers for Antennas. In Proceedings of the 2023 IEEE International Workshop on Technologies for Defense and Security (TechDefense), Rome, Italy, 20–22 November 2023; pp. 176–180. [CrossRef]
25. Longhi, M.; Vellucci, S.; Barbuto, M.; Monti, A.; Zarghani, Z.H.; Stefanini, L.; Ramaccia, D.; Bilotti, F.; Toscano, A. Circular Array Synthesis of Huygens Coatings Beamforming Metasurfaces. In Proceedings of the 2023 Seventeenth International Congress on Artificial Materials for Novel Wave Phenomena (Metamaterials), Chania, Greece, 11–16 September 2023; pp. X-208–X-210. [CrossRef]
26. Longhi, M.; Vellucci, S.; Barbuto, M.; Monti, A.; Hamzavi-Zarghani, Z.; Stefanini, L.; Ramaccia, D.; Bilotti, F.; Toscano, A. Array Synthesis of Circular Huygens Metasurfaces for Antenna Beam-Shaping. *IEEE Antennas Wirel. Propag. Lett.* **2023**, *22*, 2649–2653. [CrossRef]
27. Singh, K.; Esselle, K. Suppressing sidelobes in metasurface-based antennas using a cross-entropy method variant and full wave electromagnetic simulations. *Electronics* **2023**, *12*, 4229. [CrossRef]
28. Raana, S.; Salary, M.M.; Mosallaei, H. Broadband continuous beam-steering with time-modulated metasurfaces in the near-infrared spectral regime. *APL Photonics* **2021**, *6*, 086109.
29. Wang, P.-Y.; Rennings, A.; Erni, D. A Liquid Crystal Based Dynamic Metasurface for Beam Steering and Computational Imaging. In Proceedings of the 2020 IEEE Asia-Pacific Microwave Conference (APMC), Hong Kong, China, 8–11 December 2020; pp. 631–633. [CrossRef]
30. Vellucci, S.; Longhi, M.; Monti, A.; Barbuto, M.; Toscano, A.; Bilotti, F. Phase-Gradient Huygens' Metasurface Coatings for Dynamic Beamforming in Linear Antennas. *IEEE Trans. Antennas Propag.* **2023**, *71*, 7752–7765. [CrossRef]
31. King, R.W.P.; Fikioris, G.J.; Mack, R.B. *Cylindrical Antennas and Arrays*; Cambridge University Press: Cambridge, UK, 2002.
32. Wu, G.; Yu, W.; Lin, T.; Deng, Y.; Liu, J. Ultra-wideband RCS reduction based on non-planar coding diffusive metasurface. *Materials* **2020**, *13*, 4773. [CrossRef]
33. Carter, P.S. Antenna Arrays around Cylinders. *Proc. IRE* **1943**, *31*, 671–693. [CrossRef]

34. Cameron, T.R.; Eleftheriades, G.V. Analysis and characterization of a wide-angle impedance matching metasurface for dipole phased arrays. *IEEE Trans. Antennas Propag.* **2015**, *63*, 3928–3938. [CrossRef]
35. Lin, C.Y.; Lu, Y.S.; Lin, W.P. Design of Beamforming Phased Array Antenna for 5G Communication. In Proceedings of the 2022 10th International Japan-Africa Conference on Electronics, Communications, and Computations (JAC-ECC), Alexandria, Egypt, 19–20 December 2022; pp. 39–42. [CrossRef]
36. Yao, J.; Capmany, J.; Li, M. Microwave Photonics Beamforming Networks for Phased Array Antennas. In *Microwave Photonics*; IEEE: Piscataway, NJ, USA, 2024; pp. 237–275. [CrossRef]
37. Ribeiro, L.N.; Schwarz, S.; Rupp, M.; de Almeida, A.L.F. Energy Efficiency of mmWave Massive MIMO Precoding with Low-Resolution DACs. *IEEE J. Sel. Top. Signal Process.* **2018**, *12*, 298–312. [CrossRef]
38. Selvanayagam, M.; Eleftheriades, G.V. Discontinuous electromagnetic fields using orthogonal electric and magnetic currents for wavefront manipulation. *Opt. Express* **2013**, *21*, 14409–14429. [CrossRef] [PubMed]
39. Asadchy, V.S.; Albooyeh, M.; Tcvetkova, S.N.; Díaz-Rubio, A.; Ra'di, Y.; Tretyakov, S.A. Perfect control of reflection and refraction using spatially dispersive metasurfaces. *Phys. Rev. B* **2016**, *94*, 075142. [CrossRef]
40. Pfeiffer, C.; Grbic, A. Metamaterial Huygens' surfaces: Tailoring wave fronts with reflectionless sheets. *Phys. Rev. Lett.* **2013**, *110*, 197401. [CrossRef] [PubMed]
41. Pfeiffer, C.; Emani, N.K.; Shaltout, A.M.; Boltasseva, A.; Shalaev, V.M.; Grbic, A. Efficient Light Bending with Isotropic Metamaterial Huygens' Surfaces. *Nano Lett.* **2014**, *14*, 2491–2497. [CrossRef] [PubMed]

Disclaimer/Publisher's Note: The statements, opinions and data contained in all publications are solely those of the individual author(s) and contributor(s) and not of MDPI and/or the editor(s). MDPI and/or the editor(s) disclaim responsibility for any injury to people or property resulting from any ideas, methods, instructions or products referred to in the content.